

Multi-Dimensional Hybrid Simulation Using a Six-Actuator Self-Reaction Loading System

N. Nakata¹, B.F. Spencer, Jr.², and A.S. Elnashai²

¹ Assistant Professor, Dept. of Civil Engineering, Johns Hopkins University, Baltimore, USA

² Professor, Dept. of Civil and Env. Engineering, University of Illinois at Urbana-Champaign, Urbana, USA
Email: nakata@jhu.edu, bfs@uiuc.edu, and aelnash@uiuc.edu

ABSTRACT:

Hybrid simulation is an effective method for the assessment of the seismic response of structures, combining laboratory testing, computational analysis, and numerical time-step integration of the equations of motion. While this approach has been used for evaluation of the seismic performance of a variety of structures, applications to date have been limited to planner loading and to relatively simple structural systems. The objective of this study is to develop a multi-dimensional hybrid simulation framework using a six-actuator, self-reaction, loading system for evaluation of the seismic performance of large and complex structural systems. The framework includes the development of versatile mixed load and displacement control strategy that is critical to imposing simultaneously the gravity load in the axial direction and the earthquake-induced deformation in other directions on test specimen. To demonstrate a multi-dimensional hybrid simulation, hybrid simulation of a skew reinforced concrete (RC) bridge is conducted. In the hybrid simulation, a small-scale RC pier is tested experimentally using the mixed load and displacement control, while the rest of the piers and the bridge deck are modeled and analyzed computationally. The experimental results show that the multi-dimensional hybrid simulation with versatile six degrees-of-freedom loading capability is a promising approach that provides a reliable means for evaluation of the seismic performance of large and complex structural systems.

KEYWORDS:

Experimental Methods, Earthquake Engineering, Hybrid Simulation, Skew Bridge, Seismic Assessment

1. INTRODUCTION

Hybrid simulation combines laboratory testing, computational analysis, and numerical integration of the equations of motion to simulate dynamic response of structures. Because critical sections that are difficult to model or exhibit complex behavior are usually experimentally evaluated, simulation results provide more accurate response of structures than those in numerical analysis. Compared to quasi-static loading tests where the input loading on the structural components is predetermined, hybrid simulation can be seen as a sophisticated component test in which responses are evaluated at systems level accounting for the input ground motion. Since its initial development (Takanashi et al. 1975), a lot of effort has been made towards improvement and verification of test methods, including numerical integration algorithms (Mahin et al. 1985 and Shing et al. 1996).

While hybrid simulation has been used for evaluation of the seismic performance of a variety of structures, applications to date have been limited to planner loading and to relatively simple structural systems. In contrast, actions during strong earthquakes are three-dimensional and continuously varying. Seismic performance of structures under strong earthquakes is a highly coupled cause (action) –effect (behavior) problem. Thus, assessment of such multi-dimensionally varying actions is essential for understanding of the seismic behavior of structural components, especially for those in large and complex structural systems.

This paper reports a multi-dimensional, mixed load and displacement controlled hybrid simulation using a six-actuator, self-reaction, loading system. Following a detailed description of mixed load and displacement control strategy, six-actuator, self-reaction, loading system is introduced as a loading platform where mixed load and displacement control strategy is implemented. As an example of complex structural systems, skew RC

bridge is studied where one of the RC piers is experimentally tested and the rest of the bridge structure is computationally analyzed. Mixed load and displacement control is utilized to impose simultaneously the gravity load in the axial direction and the earthquake-induced displacement in other directions on the experimentally tested RC pier. Using the multi-dimensional hybrid simulation, seismic behavior of the RC pier under spatial loading (i.e., axial, shear, flexural, and torsional loadings) is experimentally investigated.

2. MIXED LOAD AND DISPLACEMENT CONTROL

Gravity load effects have been carefully considered in structural tests by many researchers (Kawashima et al. 2004, Lynn et al. 1996, and Pan et al. 2005). However, their test setups are combination of load-controlled actuators in the vertical direction and displacement-controlled actuators in the lateral direction of the specimen. Under large deformation, lateral actuators will have a force component in the vertical direction that should be considered.

Mixed load and displacement control in this study is defined as a combined control with either a load or displacement control in each Cartesian axis at a loading point. If a control system has coupling between actuator and Cartesian coordinates (i.e., $x, y, z, \theta_x, \theta_y, \theta_z$), mixed load and displacement control, including gravity loading and lateral displacement control, cannot be achieved with independent control of each actuator. The challenge is due to the contribution of unknown displacements in load-controlled actuator and unknown forces in displacement-controlled actuator to the target mixed load and displacement. In other words, mixed load and displacement commands cannot be explicitly decomposed into each actuator command without geometric approximation. Versatile and generally-applicable mixed load and displacement control algorithms need to be developed to take into account instantaneous and spatial coupling in the control system.

2.1. Control Algorithm

The proposed mixed load and displacement control method incorporates load-to-displacement command conversions in a mixed load and displacement control feedback loop. Figure 1 shows the main block diagrams for the proposed control method. The conversion is based on the incremental iteration process employing the Broyden (1965) update of the stiffness Jacobian of the tested structure. Because all actuator servo loops are closed with displacement output, the control system is robust for mixed-mode control.

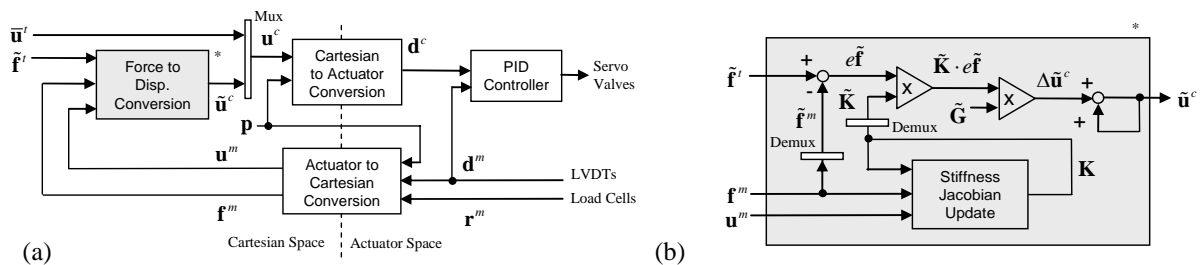


Figure 1. Block diagram for the mixed load and displacement control: (a) outer loop; and (b) force-to-displacement conversion

2.2. Iterative Procedure for the Mixed Load and Displacement Convergence

In the proposed method, target mixed load and displacement are achieved through a process that comprises directional and iterative ramps. First, the directional ramp is executed with an updated command in the displacement controlled axes whereas the command in the load control axes remains that at the end of the previous step. Then, iterative ramps are repeated with an updated command in the load controlled axes until convergence to the target load is achieved. After each ramp, an approximation of the stiffness Jacobian is updated using the Broyden's method. A single step in the mixed mode control procedure is described below:

(i) *Directional Ramp at Step N:*

$$\bar{\mathbf{u}}_{N(0)}^c = \bar{\mathbf{u}}_N^t \quad (2.1)$$

$$\tilde{\mathbf{u}}_{N(0)}^c = \tilde{\mathbf{u}}_{N-1}^c \quad (2.2)$$

where $\bar{\mathbf{u}}_{N(0)}^c$ and $\tilde{\mathbf{u}}_{N(0)}^c$ are the command displacement at the directional ramp in the N -th step in displacement- and load-controlled axes, respectively; $\bar{\mathbf{u}}_N^t$ is a target displacement in displacement controlled axes at step N ; and $\tilde{\mathbf{u}}_{N-1}^c$ is a command displacement in load controlled axes at step $N-1$.

(ii) *Update the Stiffness Jacobian After the Directional Ramp:*

$$\mathbf{K}_{N(0)} = \mathbf{K}_{N-1} + \frac{(\Delta \mathbf{f}_{N(0)}^m - \mathbf{K}_{N-1} \cdot \Delta \mathbf{u}_{N(0)}^m) \cdot (\Delta \mathbf{u}_{N(0)}^m)^T}{\|\Delta \mathbf{u}_{N(0)}^m\|^2} \quad (2.3)$$

where $\mathbf{K}_{N(0)}$ is a updated stiffness Jacobian after the directional ramp at the N -th step; $\Delta \mathbf{u}_{N(0)}^m$ and $\Delta \mathbf{f}_{N(0)}^m$ are the measured incremental displacement and load vectors, respectively, and are written as follows:

$$\Delta \mathbf{u}_{N(0)}^m = \mathbf{u}_{N(0)}^m - \mathbf{u}_{N-1}^m \quad (2.4)$$

$$\Delta \mathbf{f}_{N(0)}^m = \mathbf{f}_{N(0)}^m - \mathbf{f}_{N-1}^m \quad (2.5)$$

Eq. (2.3) is known as Broyden update of the Jacobian. It satisfies the following relationship.

$$\Delta \mathbf{f}_{N(0)}^m = \mathbf{K}_{N(0)} \Delta \mathbf{u}_{N(0)}^m \quad (2.6)$$

(iii) *Iterative Ramp at i -th Iteration at Step N:*

$$\bar{\mathbf{u}}_{N(i)}^c = \bar{\mathbf{u}}_N^t \quad (2.7)$$

$$\tilde{\mathbf{u}}_{N(i)}^c = \tilde{\mathbf{u}}_{N(i-1)}^c + \tilde{\mathbf{G}} \cdot \tilde{\mathbf{K}}_{N(i-1)} \cdot (\tilde{\mathbf{f}}_N^t - \tilde{\mathbf{f}}_{N(i-1)}^m) \quad (2.8)$$

where $\tilde{\mathbf{G}}$ is a mixed-mode gain matrix in the load-controlled axes and $\tilde{\mathbf{K}}_{N(i-1)}$ is the updated stiffness Jacobian after the i -th iteration at the N -th step in the load controlled axes.

(iv) *Update the Stiffness Jacobian After the i -th Iterative Ramp:*

$$\mathbf{K}_{N(i)} = \mathbf{K}_{N(i-1)} + \frac{(\Delta \mathbf{f}_{N(i)}^m - \mathbf{K}_{N(i-1)} \cdot \Delta \mathbf{u}_{N(i)}^m) \cdot (\Delta \mathbf{u}_{N(i)}^m)^T}{\|\Delta \mathbf{u}_{N(i)}^m\|^2} \quad (2.9)$$

where $\mathbf{K}_{N(i)}$ is an updated stiffness Jacobian after the i -th iterative ramp at the N -th step. The displacement and force increment vector $\Delta \mathbf{u}_{N(i)}^m$ and $\Delta \mathbf{f}_{N(i)}^m$ are written as follows:

$$\Delta \mathbf{u}_{N(i)}^m = \mathbf{u}_{N(i)}^m - \mathbf{u}_{N(i-1)}^m \quad (2.10)$$

$$\Delta \mathbf{f}_{N(i)}^m = \mathbf{f}_{N(i)}^m - \mathbf{f}_{N(i-1)}^m \quad (2.11)$$

(v) *Convergence Evaluation:*

$$\left| \tilde{\mathbf{f}}_N^t - \tilde{\mathbf{f}}_{N(i)}^m \right| \leq \epsilon \tilde{\mathbf{f}} \quad (2.12)$$

where $\epsilon \tilde{\mathbf{f}}$ is a load tolerance vector in the load controlled axes. If Eq. (2.12) is not satisfied, the process goes back to (iii) and is repeated until the convergence criterion is satisfied. Following convergence, the process goes to the next step $N+1$ with following relationships:

$$\tilde{\mathbf{u}}_N^c = \tilde{\mathbf{u}}_{N(i)}^c \quad (2.13)$$

$$\tilde{\mathbf{f}}_N^m = \tilde{\mathbf{f}}_{N(i)}^m \quad (2.14)$$

Because of the updating feature, the proposed method takes into account material inelasticity and geometric nonlinearity and other abrupt effects, such as cracking, in the control process. Therefore, the proposed method is robust and efficient in terms of the load control in multi-axial control systems. Most importantly, with small increments in the directional ramp, this method is capable of producing the desired mixed load and displacement load history even for path-dependent structures.

3. SIX ACTUATOR SELF-REACTION LOADING SYSTEM

The state-of-the-art six actuator self-reaction loading system, referred to as Load and Boundary Condition Box (LBCB) at the University of Illinois at Urbana-Champaign (UIUC), is used as a platform for implementing the developed control strategies and hybrid simulation in the following section. Figure 2 (a) and (b) show the full-scale and 1/5th-scale LBCBs, respectively. Both units are servo hydraulic systems each consisting of a reaction box, a loading platform and six actuators with a servo valve, load cell and LVDT. The specifications of each LBCB are summarized in Table 1.

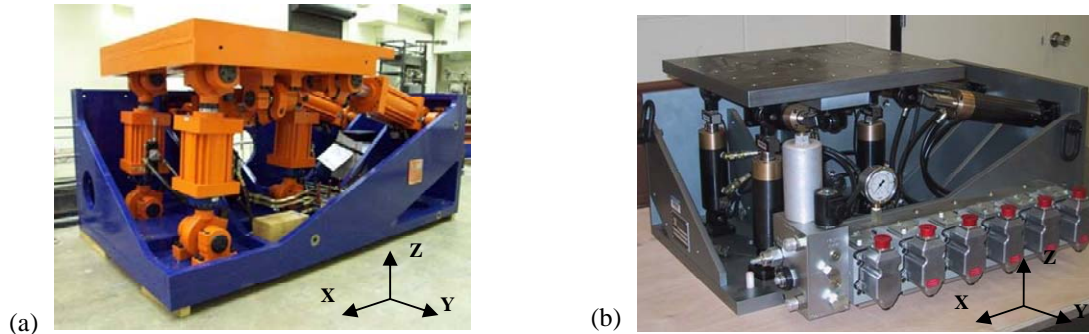


Figure 2. Load and Boundary Condition Boxes (LBCB): (a) full-scale LBCB, and (b) 1/5th-scale LBCB

Table 1. Specifications of full- and 1/5th-scale LBCBs

Full-scale LBCB					1/5 th -scale LBCB						
Displacement (mm)	x	+254	Force (kN)	x	+2402	Displacement (mm)	x	+50.8	Force (kN)	x	+8.9
	y	+127		y	+1201		y	+25.4		y	+4.5
	z	+127		z	+3603		z	+25.4		z	+12.3
Rotation (degree)	x	+16.0	Moment (kN*m)	x	+862	Rotation (degree)	x	+16.0	Moment (kN*m)	x	+1.13
	y	+11.8		y	+1152		y	+12.0		y	+2.03
	z	+16.0		z	+862		z	+16.0		z	+1.13

4. MULTI-DIMENSIONAL HYBRID SIMULATION OF SKEW RC BRIDGE

4.1. Prototype Bridge

Due to coupling of vibration responses, skew bridges are known to have complex behavior. To assess the seismic behavior of skew bridges and associated performance of RC piers, three-dimensional simulation is required to properly account for loading and boundary conditions.

Design Example No.4 (FHWA No.4 Bridge) from FHWA Seismic Design of Bridges (FHWA 1996) is selected as a prototype bridge in the following multi-dimensional hybrid simulation. Figure 3 shows the plan, elevation, and cross-sectional views of the FHWA No.4 bridge. The bridge is a three-span, continuous, concrete box girder bridge with a skew angle of 30 degree. Each bent consists of two circular reinforced concrete piers and cap beam integrated into the box girder.

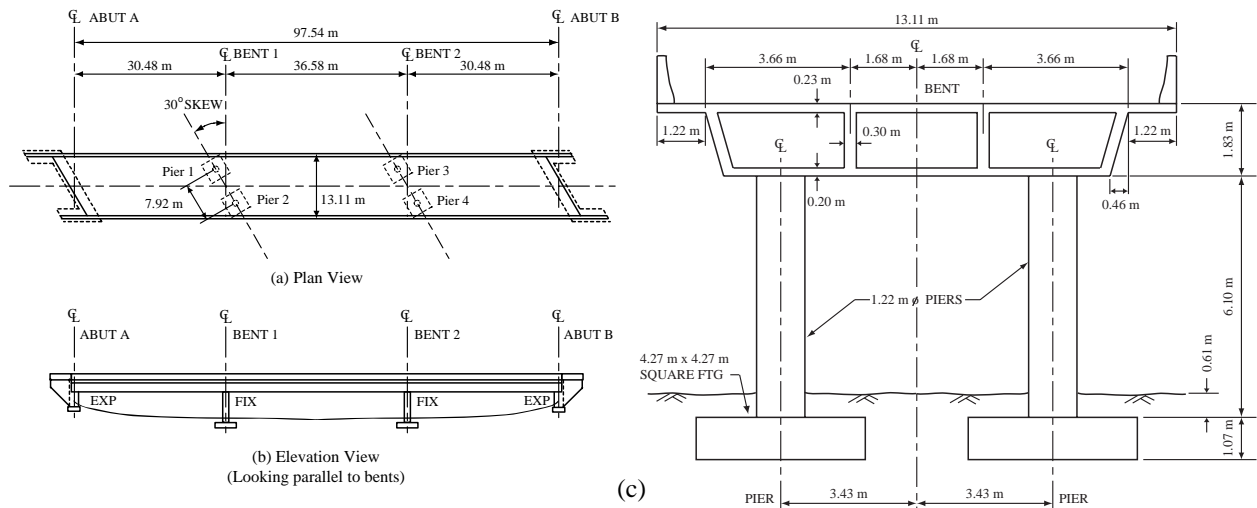


Figure 3. FHWA No.4 Bridge: (a) plan view; (b) elevation view; and cross-sectional view (Courtesy of FHWA)

4.2. Modeling and Substructures

The FHWA No.4 bridge is modeled using various elements to capture the fundamental and nonlinear behaviors. Figure 4 shows the schematic of the analytical model for the FHWA No.4 bridge.

RC piers are modeled with nonlinear fiber beam elements with cross sectional and material properties. ZeusNL is employed for the RC pier modeling. Because the superstructure usually remains elastic even during earthquake, the bridge deck, including the cap beams and end diaphragms, are modeled in linear beam elements. The bent foundations and abutment resistance are modeled as spring elements with equivalent stiffness for the spread footing and wingwall, respectively. The superstructure and foundations are modeled in Matlab. The substructuring technique is employed to combine the four RC pier substructures from ZeusNL and the rest of the structure from Matlab.

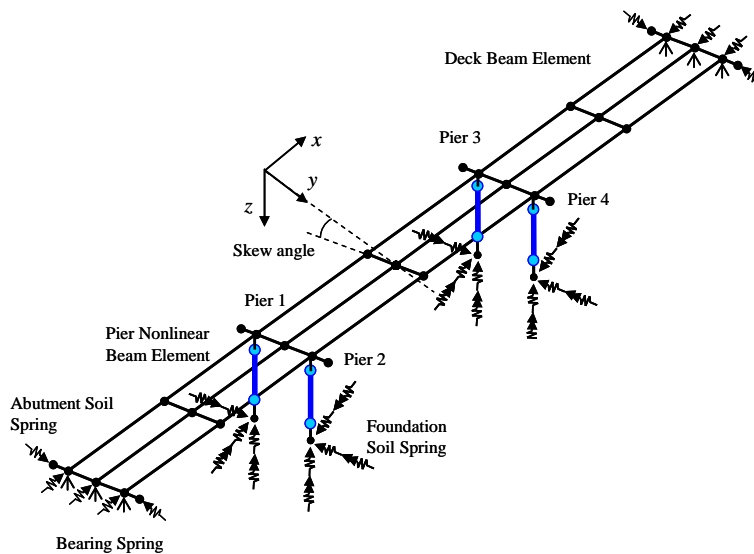


Figure 4. Modeling of the FHWA No.4 bridge

4.3. Small-scale RC Pier

In the hybrid simulation, one of the piers (Pier 4 in Figure 4) is experimentally modeled with scaling factor of 20. A small-scale RC pier is constructed with the original aspect and reinforcement ratios. Diameter and height of the specimen are 51 mm and 305 mm, respectively. Micro-concrete with a selected design mix is used for modeling of concrete at small-scale. The compressive strength of the micro-concrete mix is 31MPa. Heat-treated threaded rods and annealed steel wires are used as longitudinal and spiral transverse reinforcements. The yield strengths of the threaded rod and annealed wire are 345MPa and 414MPa, respectively.

4.4. Hybrid Simulation of Skew RC Bridge

The hybrid simulation model herein has five substructures: the bridge superstructure modeled in Matlab, three RC pier models in ZeusNL (Piers 1-3), and the small-scale RC pier model in experiment (Pier 4). Communication of all substructure models is coordinated by UI-SimCor developed at University of Illinois. The alpha-OS method with time increment of 0.01 sec is used as the time-step integration algorithm. For a loading scheme, traditional slow-rate ramp-hold loading procedure is employed.

The Morgan Hill earthquake record in 1984 at the station G06 is selected as the input ground motion. Two horizontal components of the record are considered with amplification factor. Based on the expected displacement feasible in the loading system from parametric study prior to the hybrid simulation, amplifications of the longitudinal and transverse components are determined to be 1.5 and 1.0, respectively. Figure 5 shows the amplified acceleration histories used in the hybrid simulation.

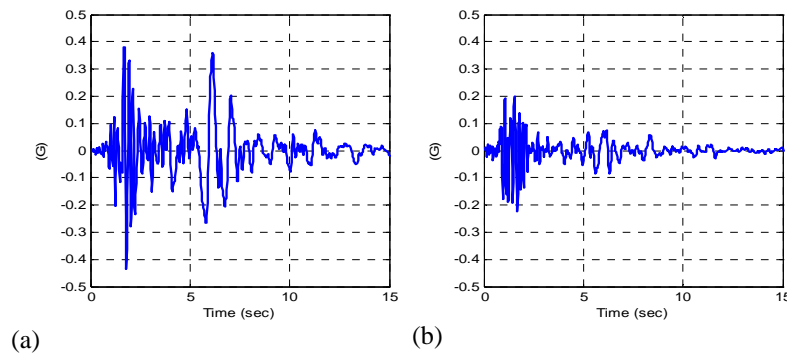


Figure 5. Input ground motion: (a) longitudinal direction, and (b) transverse direction.

4.5. Experimental Results

Hybrid simulation of the skew RC bridge is conducted using a 1/5th-scale LBCB combining mixed load and displacement control to impose constant axial load in the vertical direction and earthquake-induced displacements in the other directions on the experimentally tested RC pier. Figure 6 shows displacement and force time-histories of the RC pier. The x, y, and z-axes are in the longitudinal, transverse, and vertical directions of the bridge, respectively. Associated loading directions on the RC pier are shown in the Figure 7. As shown in the plots, the RC pier is subjected to three-dimensional deformation in all 6DOF due to the earthquake input and the gravity load effect. It is noted that the axial force in the z-axis remains constant at the initial gravity load level during the simulation regardless of the displacement in other five directions. The combined action of gravity load in axial direction and earthquake-induced deformation in other five directions on the RC pier is successfully achieved by the mixed load and displacement control capability. The variation in the axial displacement is a result of control of the axial force. This peculiar behavior cannot be simulated without the mixed load and displacement control capability.

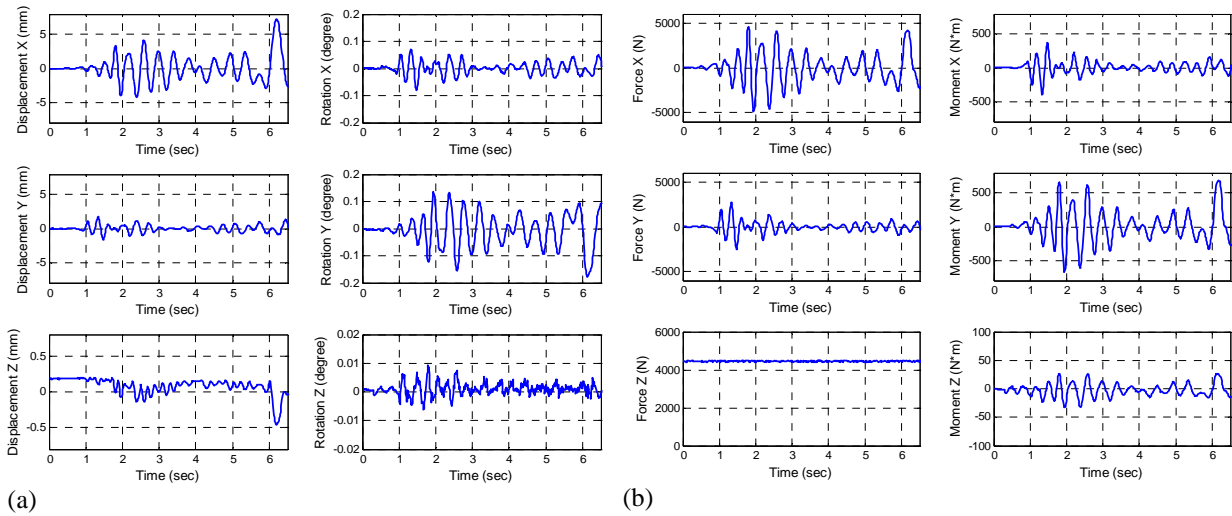


Figure 6. Displacement and force time-histories: (a) displacements and rotations, and (b) forces and moments.

In-plane displacement trajectories are shown in Figure 7. These plots indicate a displacement path at the top of the RC pier in three-dimensional space. Figure 8 shows displacement and force relationships in the longitudinal and transverse directions. The longitudinal response exhibits an inelastic hysteresis loop including yielding and post-peak behavior. Although the transverse response does not exhibit significant inelastic behavior, the transverse stiffness reduces by about 50% after the peak strength in the longitudinal direction is reached. This result is due to the interaction between the longitudinal and transverse behaviors. Interactions among multiple directional behaviors cannot be evaluated in a simple in-plane simulation. As such, accounting for realistic loadings and boundary conditions is important for the assessment of seismic performance of critical structural components.

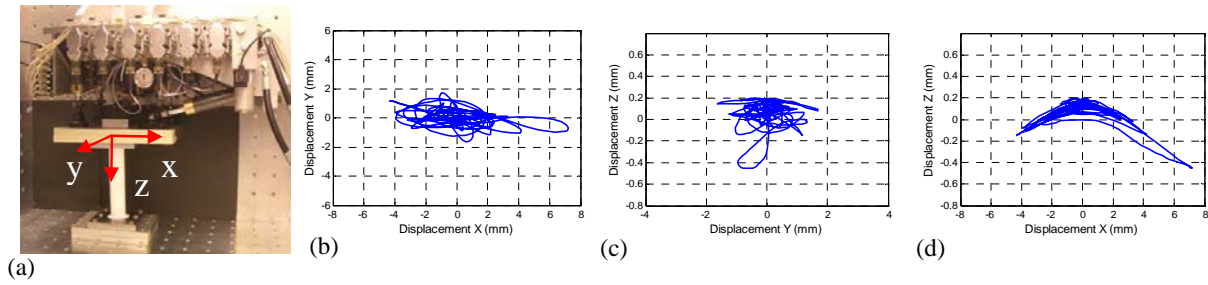


Figure 7. In-plane displacement trajectories: (a) loading coordinates, (b) x-y plane, (c) y-z plane, and (d) x-z plane.

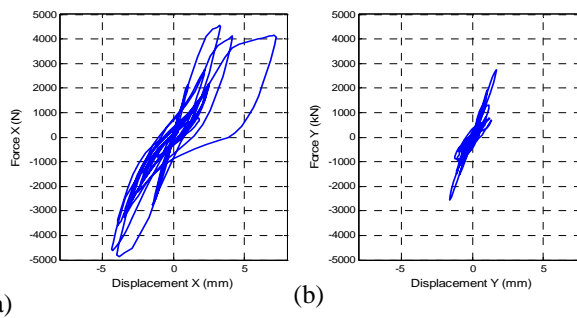


Figure 8. Displacement-force relationships: (a) longitudinal direction, and (b) transverse direction.

5. CONCLUSIONS

The paper presents the application of the multi-dimensional, mixed load and displacement controlled hybrid simulation using a six-actuator, self-reaction, loading system to the complex structural systems. As an example of the complex structural systems, skew RC bridge is investigated using the hybrid simulation method where an RC pier is experimentally tested and the rest of the bridge structure is computationally analyzed. The mixed load and displacement control is used to impose the gravity load in the axial direction and the earthquake-induced displacements in the other directions on the RC pier. The experimental results show that the multi-dimensional hybrid simulation with versatile mixed load and displacement control capability is a promising approach that provides a reliable means for evaluation of the seismic performance of large and complex structural systems. Currently, a series of large-scale hybrid simulations using the full-scale LBCB are underway at UIUC. The same hybrid simulation methodology and control strategies presented in this study can be used for those large-scale experiments. Thus, the study presented in this paper lays the foundation for and provides smooth transition to the large-scale hybrid simulation including multi-dimensional simulation of complex structural systems.

ACKNOWLEDGEMENTS

This research described in the paper is supported by the George E. Brown, Jr. Network for Earthquake Engineering Simulation (NEES) Program (NSF Award No. CMS-0217325) funded by the National Science Foundation (NSF) and the Mid-America Earthquake Center, an Engineering Research Center funded by the National Science Foundation under cooperative agreement reference EEC 97-01785.

REFERENCES

- Broyden, C.G., (1965). A class of methods for solving nonlinear simultaneous equations. *Math. Comp.* 19, 577-593.
- Federal Highway Administration, (1996). Seismic Design of Bridges -Design Example No.4 Three-Span Continuous CIP Concrete Bridge. *FHWA-SA-97-009*, Federal Way, Washington.
- Kawashima, K., Gakuho, W., Nagata, S., and Ogimoto, H., (2004). Effect of Bilateral Excitation of the Seismic Performance of Reinforced Concrete Bridge Columns. *Japan-Europe Seismic Risk Workshop*, University of Bristol, UK.
- Kwon, O. S., Nakata, N., Elnashai, A. S., and Spencer, B. F., (2005). A Framework for Multi-Site Distributed Simulation and Application to Complex Structural Systems. *Journal of Earthquake Engineering*, 9(5), 741-753.
- Lynn, A.C., Moehle, J.P., Mahin, S.A., and Holmes, W.T., (1996). Seismic Evaluation of Existing Reinforced Concrete Building Columns. *Earthquake Spectra*, 12(4), 715-739.
- Mahin, S.A., and Shing, P.B. (1985). Pseudodynamic Method for Seismic Performance Testing. *Journal of Structural Engineering*, 111(7), 1482-1503.
- Nakata, N., Spencer, B. F., and Elnashai, A. S. (2004). Mixed Load / Displacement Control Strategy for Hybrid Simulation. *4th International Conference on Earthquake Engineering*, Taipei, Taiwan.
- Pan, P., Nakashima, M., and Tomofuji, H., (2005). Online test using displacement-force mixed control. *Earthquake Engineering and Structural Dynamics*, 34, 869-888.
- Shing, P.B., Nakashima, M., and Bursi, O.S. (1996). Application of Pseudodynamic Test Method to Structural Research. *Earthquake Spectra*, 12(1), 29-56.
- Takanashi, K., Udagawa, K., Seki, M., Okada, T., and Tanaka, H. (1975). Nonlinear Earthquake Response Analysis of Structures by a Computer-Actuator On-Line System. *Bulletin of Earthquake Resistant Structure Research Center 8*, Institute of Industrial Science, University of Tokyo.